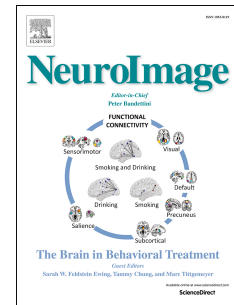


Accepted Manuscript



Oscillatory networks of high-level mental alignment: A perspective-taking MEG study

R.A. Seymour, H. Wang, G. Rippon, K. Kessler

PII: S1053-8119(18)30414-2

DOI: [10.1016/j.neuroimage.2018.05.016](https://doi.org/10.1016/j.neuroimage.2018.05.016)

Reference: YNIMG 14941

To appear in: *NeuroImage*

Received Date: 23 February 2018

Revised Date: 16 April 2018

Accepted Date: 4 May 2018

Please cite this article as: Seymour, R.A., Wang, H., Rippon, G., Kessler, K., Oscillatory networks of high-level mental alignment: A perspective-taking MEG study, *NeuroImage* (2018), doi: 10.1016/j.neuroimage.2018.05.016.

This is a PDF file of an unedited manuscript that has been accepted for publication. As a service to our customers we are providing this early version of the manuscript. The manuscript will undergo copyediting, typesetting, and review of the resulting proof before it is published in its final form. Please note that during the production process errors may be discovered which could affect the content, and all legal disclaimers that apply to the journal pertain.

Oscillatory Networks of High-Level Mental Alignment: A Perspective-Taking MEG Study

⁴ Seymour, R.A^{1,2,3}., Wang, H¹., Rippon, G¹., & Kessler, K¹.

5

⁶ ¹Aston Brain Centre, School of Life and Health Sciences, Aston University, Birmingham, B4

⁷ET. ²ARC Centre of Excellence in Cognition and Its Disorders, Macquarie University,

8 Sydney, Australia, 2109.³Department of Cognitive Science, Macquarie University, Sydney,
9 Australia, 2109.

10

11 Correspondence: Klaus Kessler (k.kessler@aston.ac.uk)

12 School of Life and Health Sciences

13 Psychology, Aston Brain Centre

14 Aston University

15 Aston Triangle

16 Birmingham, B4 7ET

17 Phone: +44 (0)121 204 3187

18

ACCEPTED MANUSCRIPT

20 **Highlights**

- 21 • Oscillatory basis of embodied perspective-taking investigated using MEG
22 • We replicate the crucial role of theta-band (3-6Hz) oscillations in perspective-taking
23 • Theta power localised to right temporo-parietal junction (rTPJ), lateral PFC and ACC
24 • Lateral PFC and ACC exert top-down influence (Granger causality) over rTPJ
25 • rTPJ increases its theta-band phase coupling to mentalizing and body schema networks

26

27 **Abstract**

28 Mentally imagining another's perspective is a high-level social process, reliant on
29 manipulating internal representations of the self in an embodied manner. Recently Wang et
30 al. (2016) showed that theta-band (3-7Hz) brain oscillations within the right temporo-parietal
31 junction (rTPJ) and brain regions coding for motor/body schema contribute to the process of
32 perspective-taking. Using a similar paradigm, we set out to unravel the extended functional
33 brain network in detail. Increasing the angle between self and other perspective was
34 accompanied by longer reaction times and increases in theta power within rTPJ, right lateral
35 pre-frontal cortex (PFC) and right anterior cingulate cortex (ACC). Using Granger-causality,
36 we showed that lateral PFC and ACC exert top-down influence over rTPJ, indicative of
37 executive control processes required for managing conflicts between self and other
38 perspectives. Finally, we quantified patterns of whole-brain phase coupling in relation to the
39 rTPJ. Results suggest that rTPJ increases its theta-band phase synchrony with brain regions
40 involved in mentalizing and regions coding for motor/body schema; whilst decreasing
41 synchrony to visual regions. Implications for neurocognitive models are discussed, and it is
42 proposed that rTPJ acts as a 'hub' to route bottom-up visual information to internal
43 representations of the self during perspective-taking, co-ordinated by theta-band oscillations.

44

45 **Keywords**

46 perspective taking; social cognition; MEG; theta; oscillations; synchrony.

47

48 **Introduction**

49 Humans possess highly developed social skills that allow us to imagine what others might be
50 experiencing, thinking or feeling to an extent not shared by other species (Tomasello et al.
51 2005). The question of what separates us from other species has been the subject of
52 substantial research in comparative psychology and cognitive neuroscience, and while
53 significant headway has been made with respect to what skills make us special (Call and
54 Tomasello 1999; Povinelli et al. 2000; Frith and Frith 2007) and which parts of our brain
55 have evolved to cope with sophisticated “mentalizing”, i.e., reading of others’ minds
56 (Lieberman 2007; Van Overwalle and Baetens 2009), much less is known about the actual
57 brain network dynamics that implement these social skills. Here we set out to investigate the
58 large-scale, distributed but synchronised neural activity that gives rise to a person’s
59 understanding of another’s visuospatial experience of the world: a process termed perspective
60 taking.

61

62 Mentally imagining another’s perspective is a high-level social process, but recent
63 behavioural experiments suggest that perspective-taking is still grounded in the cortical
64 posture and action representations of the observer. Using posture manipulations, several
65 studies (Kessler and Rutherford 2010; Kessler and Thomson 2010; Surtees et al. 2013; Wang
66 et al. 2016; Gooding-Williams et al. 2017) have shown that perspective-taking engages large
67 parts of the neuronal bases of the body schema, i.e. the cortical correlates of the internal
68 representation of the body (Coslett et al. 2008; Medina et al. 2009), in the form of a simulated
69 rotation of the embodied self into another’s orientation and perspective (Kessler and

70 Thomson 2010; Surtees et al. 2013; Wang et al. 2016). In other words, humans literally “put
71 themselves” into another’s viewpoint to understand their perspective.

72

73 Note that such embodied perspective-taking must be distinguished from so-called perspective
74 *tracking*. While both processes involve judgements about another’s perspective, perspective-
75 tracking, in contrast to perspective-taking, merely requires an observer to understand what
76 another can or cannot perceive (e.g. what is occluded and what is visible to them). The two
77 forms of perspective processing have been related to different developmental stages (Flavell
78 et al. 1981; Gzesh and Surber 1985; Moll and Tomasello 2006)
79 (perspective-tracking: ~2 years; perspective-taking ~ 4-5 years) and perspective-tracking, in
80 contrast to perspective-taking, has been observed in other species such as apes and corvids
81 (Bugnyar et al. 2004; Bräuer et al. 2007). Finally, while perspective-taking engages an
82 embodied mental rotation of the self into another’s viewpoint, perspective-tracking seems to
83 rely on inferring another’s line of sight, in other words, whether their line of sight towards a
84 target is disrupted or not (Zacks and Michelon 2005; Kessler and Rutherford 2010; Wang et
85 al. 2016).

86

87 The neural correlates of embodied simulation during perspective-taking were recently
88 investigated by Wang et al. (2016) using Magnetoencephalography (MEG, Expt. 1) and
89 converging effects were found in the right posterior temporo-parietal junction (pTPJ) for
90 cognitive effort of perspective-taking (amount of angular disparity between self vs. other’s
91 viewpoint) and for embodied processing (posture congruence) during perspective-taking (but
92 not for tracking). The crucial role of right pTPJ for perspective-taking was further confirmed
93 via transcranial magnetic stimulation (TMS) interference (Wang et al. 2016). The authors
94 further reported that low frequency theta oscillations (3-7 Hz) were the prominent neural

95 code in pTPJ, whilst Gooding-Williams et al. (2017) used repetitive TMS entrainment over
96 pTPJ to show that TMS pulses administered at theta frequency (6Hz) accelerated perspective-
97 taking, while alpha (10Hz) entrainment slowed perspective-taking down. TPJ-theta could
98 therefore be the relevant neural frequency to enable phase-coupling within a wider
99 mentalizing network.

100

101 These results build upon a perspective-taking EEG study which found an evoked component
102 at 450ms, localised primarily to the right TPJ (McCleery et al. 2011). Furthermore, they are
103 consistent with the neural correlates of perspective-taking reported using fMRI – two meta-
104 analyses (Van Overwalle 2009, 2011) have suggested that the core areas of activation include
105 bilateral TPJ and ventro-medial pre-frontal cortex (vmPFC). The posterior division of the TPJ
106 (Igelström and Graziano 2014; Bzdok et al. 2013) in particular, has been reliably linked to
107 perspective-taking and more generally to “mentalizing” (representing other’s mental states)
108 (Van Overwalle 2011; Schurz et al. 2013), as well as to so-called spontaneous “out-of-body
109 experiences” (OBE) (Blanke et al. 2005). During an OBE individuals experience the
110 sensation that the self has moved to a different physical location than their body, and this
111 sensation often entails a translation as well as a rotation of perspective, similar to a deliberate
112 perspective transformation during perspective-taking (Kessler and Braithwaite 2016). The
113 involvement of TPJ in OBEs (Blanke et al. 2005) is of importance, as it corroborates the
114 proposed link between embodied processing and high-level social mentalizing in TPJ (Blanke
115 et al. 2005; Lombardo et al. 2010; Kessler and Braithwaite 2016; Wang et al. 2016).

116

117 Whilst the TPJ is clearly important for embodied processing and perspective-taking, the
118 region is also implicated in a range of cognitive operations, including spatial attention, social
119 cognition and self/other distinctions. It has been suggested that more generally, the region

120 acts as a major hub for information integration (Igelström and Graziano 2017.; Eddy 2016),
121 especially during higher-level cognitive processes relying upon internal representations, such
122 as perspective-taking (Igelström and Graziano 2017.; Eddy 2016; Wang et al. 2016;
123 Gooding-Williams et al. 2017). Indeed, the TPJ has extensive functional connectivity to
124 many networks of the brain, including the fronto-parietal control (Vincent et al. 2008),
125 default mode (Mars et al. 2012), and ventral attention networks (Bzdok et al. 2013). We
126 therefore hypothesised that the TPJ contributes to the process of embodied transformation
127 through changes in patterns of whole-brain functional connectivity, via theta-band synchrony,
128 as would be predicted from the region's role as a network hub (Igelström and Graziano
129 2017.; Carter and Huettel 2013; Eddy 2016). However, investigations of perspective-taking
130 using connectivity analysis, e.g. in form of frequency-specific phase-coupling, are scarce. To
131 our knowledge, only one study to date (Bögels et al. 2015) has reported enhanced theta
132 phase-coherence between right TPJ and ventromedial prefrontal cortex (vmPFC) in a
133 condition that required participants to imagine another's visual experience. The major aim of
134 the current study was therefore to consolidate the crucial role of pTPJ theta oscillations in
135 perspective-taking by means of advanced network analyses.

136
137 In addition to the TPJ, Wang et al., reported increases in theta-band power for the lateral PFC
138 during the cognitive effort of perspective-taking (Wang et al. 2016). Activity within this
139 region during social cognition has been argued to reflect high-level reasoning and working
140 memory processes recruited more generally during complex perspective-taking and
141 mentalizing tasks (Van Overwalle 2011). However, there is emerging evidence that frontal
142 activity in lateral PFC but also in the anterior cingulate cortex (ACC) could play a more
143 nuanced role in perspective-taking by managing the conflict between self and other
144 perspectives (Samson et al. 2005; Bögels et al. 2015; Hartwright et al. 2015). For example

145 (McCLEERY et al. 2011) found late a (0.8-1.0s) frontal evoked response during perspective-
146 taking dependent on whether self perspective was consistent with an avatar's perspective . In
147 terms of theta-oscillations, this could potentially manifest as a direct connection between
148 lateral PFC and the core mentalizing network (Bögels et al. 2015) in TPJ and vmPFC (Van
149 Overwalle 2009, 2011). We were therefore interested in whether the TPJ becomes
150 functionally connected to various frontal and midline regions during perspective-taking
151 (Hartwright et al. 2015), and crucially determining the direction of this connectivity.

152

153 In conclusion, we set out to consolidate previous findings regarding the crucial role of TPJ
154 theta oscillations for generating the abstract social representations required for perspective-
155 taking (Bögels et al. 2015; Wang et al. 2016; Gooding-Williams et al. 2017), while
156 unravelling in detail the involved functional network in terms of dynamic oscillatory
157 coupling between brain areas, using MEG. Based on the considerations above, we expected
158 TPJ and (v)mPFC to form a mentalizing network synchronised via theta oscillations, related
159 to generating the abstract representation of another's perspective, while activation in parietal
160 body-schema areas and sensorimotor cortex would reflect the required embodied
161 transformation to generate this representation via rotation of the egocentric perspective
162 (Kessler and Rutherford 2010; Kessler and Thomson 2010; Surtees et al. 2013). In addition,
163 pACC and lPFC might play key roles in top-down executive control of the underlying
164 embodied transformation and in managing the conflict between physical self and transformed
165 self at the representational level.

166

167 Materials and Methods

168

169 *Participants*

170 Data were collected from 18 participants (4 male, 14 female, mean age = 27.55, SD = 5.86).
171 All participants had normal or corrected to normal vision and no history of neurological or
172 psychiatric illness. All experimental procedures complied with the Declaration of Helsinki
173 and were approved by the Aston University, Department of Life & Health Sciences ethics
174 committee. Written consent was obtained from all participants.

175

176 *Experimental Paradigm and Design*

177 The paradigm was adopted from a behavioural study by Kessler and Rutherford (2010). The
178 stimuli were coloured photographs (resolution of 1024×768 pixels), showing an avatar
179 seated at a round table shown from one of four possible angular disparities (see Fig. 1, left:
180 60° , 160° clockwise and anticlockwise). In each trial one of the grey spheres on the table
181 turned red indicating this sphere as the target. From the avatar's viewpoint, the target could be
182 either visible or occluded (VO) by a centrally resented black screen; or to the left or to the
183 right (LR) inducing perspective-tracking or perspective-taking, respectively. Stimuli were
184 presented in 12 mini-blocks of 32 trials, alternating between LR and VO conditions. On each
185 trial participants were asked to make a target location judgement according to the avatar's
186 perspective by pressing the instructed key on an MEG-compatible response pad: the left key
187 for "left" or "visible" targets from the avatar's viewpoint and the right key for "right" or
188 "occluded" targets. Accuracy feedback was provided after each trial in the form of a short
189 tone. As in Kessler and Rutherford (2010), we collapsed across clockwise and anticlockwise
190 disparities, and separately collapsed correct responses for left and right and visible and
191 occluded, respectively. This resulted in four separate experimental conditions (for two
192 examples see Fig. 1, left): left/right judgements where the avatar is 160° from own
193 perspective (LR-160); left-/right judgements where the avatar is 60° from own perspective
194 (LR-60); visible/occluded judgments where the avatar is 160° from own perspective (VO-

195 160); visible/occluded judgments where the avatar is 60° from own perspective (VO-60).
196 This 2x2 design allowed us to disentangle perspective-taking from perspective-tracking and
197 investigate the effect of an increased angle of disparity (we chose to use 160° vs. 60° based
198 on the results of Wang et al., 2016), between self-perspective and other-perspective, which
199 has been shown to lengthen reaction times during perspective-taking (Kessler and Rutherford
200 2010; Surtees et al. 2013).

201

202 *Behavioural Data Analysis*

203 Behavioural reaction times (RT) from the experimental paradigm were extracted from E-
204 Prime® data files and converted to .csv format. Data from two participants with MEG
205 movement over 5mm was discarded. All trials containing incorrect answers or response times
206 greater than 2 standard deviations from the median were excluded from subsequent analyses.
207 For the four experimental conditions (LR-160; LR-60; VO-160; VO-60), median RT from
208 each participant were entered into a one-way ANOVA using the JASP statistics package.

209

210 *MEG and Structural MRI Acquisition*

211 MEG data were acquired using a 306-channel Neuromag MEG scanner (Vectorview, Elekta,
212 Finland) made up of 102 triplets of two orthogonal planar gradiometers and one
213 magnetometer. All recordings were performed inside a magnetically shielded room at a
214 sampling rate of 1000Hz. Five head position indicator (HPI) coils were applied for
215 continuous head position tracking, and visualised post-acquisition using an in-house Matlab
216 script. Two participants had excessive head movement (>5mm), and were excluded from
217 subsequent analyses. For MEG-MRI coregistration purposes three fiducial points, the
218 locations of the HPI coils and 300-500 points from the head surface were acquired using the
219 integrated Polhemus Fastrak digitizer. Visual stimuli were presented on a projection screen

220 located 86cm from participants, and auditory feedback through MEG-compatible
221 headphones. Data acquisition was broken down into three sequential runs, each lasting 8-10
222 minutes.

223

224 A structural T1 brain scan was acquired for source reconstruction using a Siemens
225 MAGNETOM Trio 3T scanner with a 32-channel head coil (TE=2.18ms, TR=2300ms,
226 TI=1100ms, flip angle=9°, 192 or 208 slices depending on head size, voxel-size =
227 0.8x0.8x0.8cm).

228

229 *MEG Preprocessing*

230 All MEG data were pre-processed using Maxfilter (temporal signal space separation, .96
231 correlation), which suppresses external sources of noise from outside the head (Taulu and
232 Simola 2006). To compensate for head movement between runs, data from runs 2 and 3 were
233 transformed to participant's head position at the start of the first block using the *-trans* option
234 of Maxfilter. For each participant, the entire recording was band-pass filtered between 0.5-
235 250Hz (Butterworth filter) and band-stop filtered to remove residual 50Hz power-line
236 contamination and its harmonics. Data were then epoched into segments of 2500ms (1000ms
237 pre, 1500post stimulus onset) and each trial was demeaned and detrended. Trials containing
238 artefacts (SQUID jumps, eye-blanks, head movement) were removed by visual inspection,
239 resulting in removal of an average of 6.14% of trials per condition, per participant (additional
240 descriptive statistics reported in Table S1). For sensor-level analyses, ICA was used to
241 identify and reduce residual EOG and ECG artefacts. Four MEG channels containing large
242 amounts of non-physiological noise were removed from all source-level analyses. The pre-
243 processed data were then separated into the four experimental conditions and downsampled
244 to 250Hz to aid computation time.

245

246 *MEG-MRI Coregistration*

247 MEG data were co-registered with participants' T1 MRI structural scan by matching the
248 digitised head shape data with surface data from the structural scan (Jenkinson and Smith
249 2001). Subsequently, the aligned MRI-MEG image was used to create (i) a forward model
250 based on a single-shell description of the inner surface of the skull (Nolte 2003), using the
251 segmentation function in SPM8 and (ii) spatial normalisation parameters to create individual
252 volumetric grids. To facilitate group analysis, each individual volumetric grid was warped to
253 a template based on the MNI brain (8mm resolution). Subsequently the inverse of the
254 normalisation parameters were applied to the template grid, for source analysis.

255

256 *Sensor Level Analysis*

257 Sensor-level time-frequency representations (TFRs) were calculated using a single Hanning
258 taper between frequencies of 1-30Hz in steps of 1Hz. The entire 2500ms epoch was used,
259 with a sliding window of 500ms, but the first 250ms and last 500ms of each trial were
260 discarded to avoid edge artefacts. Due to different scales between the two MEG sensor-types,
261 only data from the gradiometers were used, with TFR power averaged across each pair post-
262 hoc. All analyses were computed on single trials and subsequently averaged, and therefore
263 TFRs contain both phase-locked (evoked) and non phase-locked (induced) information. As
264 hypothesised from previous research using a similar paradigm (Wang et al. 2016), TFR
265 responses averaged across subjects showed prominent differences between conditions within
266 the theta-band (2-7Hz).

267

268 For statistical testing, we therefore compared theta-band (2-7Hz), alpha (8-12Hz) and beta
269 (13-30Hz) power during trials in which the avatar was 160^0 versus 60^0 from the participant's

270 own perspective (clockwise or anticlockwise), in both left/right judgements (i.e. perspective-
 271 taking), and visible/occluded judgements (i.e. perspective-tracking). We corrected for
 272 multiple comparisons across time, frequency and space via cluster-based non-parametric
 273 permutation testing (Maris and Oostenveld 2007). Results showed a significant cluster of
 274 greater (3-6Hz) theta-band power at 0-650ms in the LR-160 versus LR-60 condition
 275 (highlighted in Fig S1, left), but not for VO-160 vs. VO-60, (Fig. S1, right).

276

277 *MEG Source-Level*

278 Source localisation was conducted using Dynamical Imaging of Coherent Sources (Gross et
 279 al. 2001) (DICS) which applies a spatial filter to the MEG data at every voxel of a canonical
 280 0.8 cm brain-grid, in order to maximise signal from that location whilst attenuating signals
 281 elsewhere. The spatial filter was calculated from the cross-spectral densities for a time–
 282 frequency tile centred on the effects found at sensor level (3-6Hz; 0–650ms; gradiometer
 283 channels only; see Fig. 1, top-right; Supplementary Figure S1). For all analyses, a common
 284 filter across baseline and active periods was used and a regularisation parameter of lambda
 285 5% was applied. Cluster-based non-parametric permutation testing was used to correct for
 286 multiple comparisons across voxels (Maris and Oostenveld 2007), for the LR-160>LR-60
 287 and VO-160>VO-60 contrasts. The resulting whole-brain statistical maps were spatially
 288 smoothed using a robust smoothing algorithm (Garcia 2010) as implemented in bspmview,
 289 and presented on a 3D cortical mesh using the Connectome Workbench software (Van Essen
 290 et al. 2012). Using the spatial filters computed during source analysis, we extracted trial-by-
 291 trial time-courses from three regions of interest, as shown in Fig. 2A, using the MNI co-
 292 ordinates with the highest t-value within each region (Table S3).

293

294 *Granger Causality Analysis*

295 The directed functional connectivity between these three ROIs was estimated using
 296 spectrally-resolved non-parametric Granger causality (Dhamala et al. 2008) as implemented
 297 in the Fieldtrip toolbox (Oostenveld et al. 2010). Intact and scrambled time-series were split
 298 into 0.325s epochs to enhance the accuracy of the results (0-0.65s post stimulus onset),
 299 followed by Fourier transformation (Hanning taper; 2Hz spectral smoothing), before being
 300 entered into a non-parametric spectral matrix factorisation procedure. Granger causality was
 301 then estimated between each ROI pair and each ROI-scrambled time-series. Statistical
 302 analysis was performed using cluster-based permutation testing (Maris and Oostenveld
 303 2007). Granger causal influence between two regions (A & B) was deemed significant if
 304 values were i) significantly greater than scrambled data ($p < .05$) and ii) significantly greater in
 305 one direction than another (i.e. A-to-B versus B-to-A, $p < .05$).

306

307 *Theta-band Imaginary Coherence*

308 To estimate patterns of whole-brain connectivity supporting high-level perspective taking,
 309 mediated by the right TPJ, we quantified theta-band phase synchrony during LR-160 trials
 310 compared with LR-60 trials. A complex-valued spectral estimate at 5 ± 2 Hz for each grid-
 311 point was estimated using an adaptive spatial filter [the ‘PCC’ method, as implemented in
 312 *ft_sourceanalysis* (Oostenveld et al. 2010)]. Coherence was used to quantify the phase
 313 consistency between a seed region in TPJ (MNI co-ordinates [40 -58 36]) and every other
 314 voxel of the canonical 0.8 cm brain-grid, using *ft_connectivityanalysis* (Oostenveld et al.
 315 2010). Coherence values are normalised to range from 0 (no phase synchrony) to 1
 316 (completely phase synchronised). We opted to project the complex-valued coherency
 317 estimates onto the imaginary axis, as suggested by Nolte et al., (Nolte et al. 2004). This
 318 removes estimates of instantaneous phase, thereby reducing the influence of spurious
 319 connectivity resulting from MEG field spread (Nolte et al. 2004), but comes at the expense of

320 removing genuine connectivity at zero-lag. Further details on the quantification of
321 “imaginary coherence” can be found elsewhere (Nolte et al. 2004; Oostenveld et al. 2010).
322 Whole-brain coherence maps from LR-160 and LR-60 trials were baseline-corrected and
323 compared using cluster-based permutation-testing as implemented in the Fieldtrip toolbox
324 (Oostenveld et al. 2010). The resulting whole-brain statistical maps were spatially smoothed
325 using a robust smoothing algorithm (Garcia 2010) as implemented in bspmview, and
326 presented on a 3D cortical mesh using the Connectome Workbench software (Van Essen et
327 al. 2012).

328

329 *Supplementary Methods and Analysis Code*

330 Additional details are provided in SI Materials and Methods. MATLAB code for all analyses
331 is openly available online at
332 https://github.com/neurofractal/perspective_taking_oscillatory_networks (Seymour 2017).

333

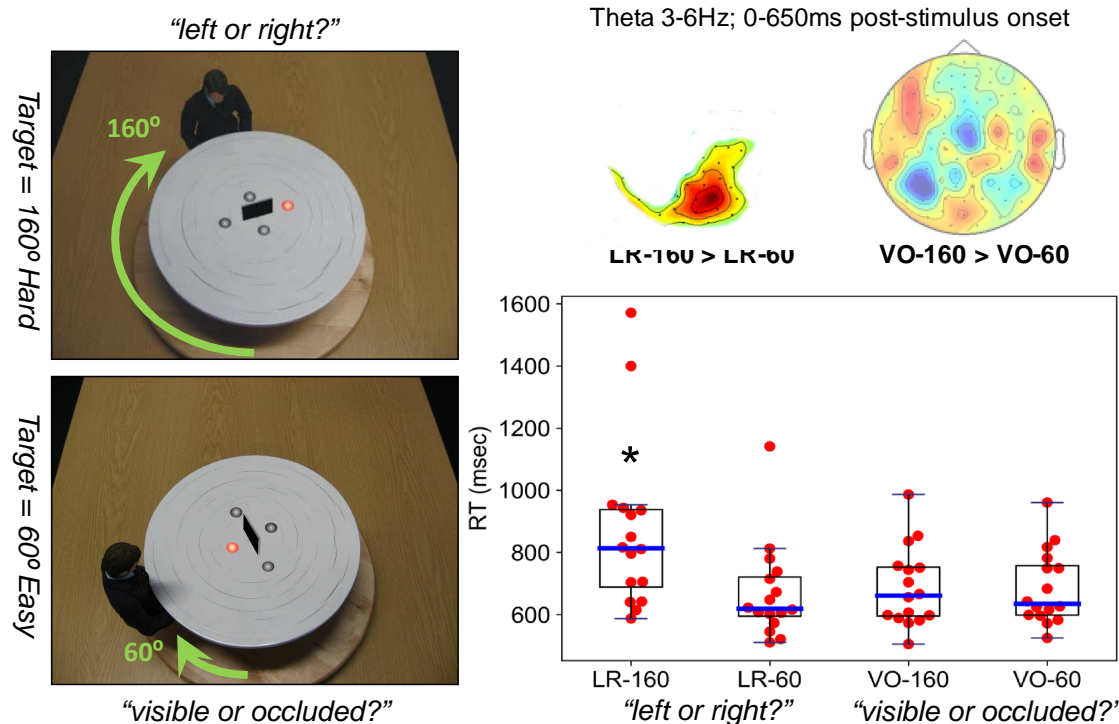
334 **Results**

335

336 *Behavioural Results*

337 For the four experimental conditions, median reaction times (RT) from each participant were
338 entered into a one-way ANOVA (output detailed in Table S2). Results showed a main effect
339 of experimental condition on RT, $F(3,60) = 4.43$, $p=.007$, $\eta^2 = 0.181$. Post-hoc tests revealed
340 this was due to significantly longer RT for the LR-160 conditions compared with all other
341 conditions (LR-60, $p_{tukey} = .013$; VO-160, $p_{tukey} = .029$; VO-60, $p_{tukey} = .026$), replicating
342 Kessler and Rutherford (2010). The raw statistical output is reported in Table S2.

343



344

345 *Figure 1.* Left: Experimental paradigm (Kessler and Rutherford 2010) showing two example
 346 stimuli (see Materials and Methods for details). Bottom right: Boxplot of participants' (N =
 347 16, 2 participants removed with excess head movement) median reaction time (RT) in
 348 milliseconds for the two angular disparity conditions (160 vs. 60) of perspective-taking (L/R)
 349 and perspective-tracking (V/O), respectively. * = LR-160 is significantly different from all
 350 other conditions ($p < .05$). Top right: Sensor-level topoplots of theta activity (3-6Hz), showing
 351 a significant cluster (high visibility) for perspective-taking but not for perspective-tracking
 352 (further details in Materials and Methods and supplementary information).

353

354 *Task-Related Changes in Theta Power*

355 Using a data-driven approach from 2-30Hz, time-frequency results at the sensor-level (see
 356 Fig. 1 and Fig. S1) replicated the crucial role of theta oscillations in perspective-taking
 357 (Wang et al. 2016; Gooding-Williams et al. 2017). A significant positive cluster ($p = 0.03$) was
 358 found at 3-6Hz, 0-650ms, when comparing angular disparities of 160° and 60° degrees for

359 the L/R task. No significant effects were found for any other frequencies ($p>.05$). In addition,
360 no significant clusters were found for the V/O task, i.e. perspective-tracking in the VO-160 vs
361 VO-60 contrast.

362

363 [Inline supplementary material - Insert Figure S1 here]

364

365 Based on these sensor-level data, which replicate our previous study (Wang et al., 2016), we
366 decided to concentrate on further characterising theta-band power and connectivity
367 underlying perspective-taking. Whilst a wider frequency range, that also included higher
368 delta frequencies, has been used to define theta-band power in previous studies (Wang et al.
369 2016), we opted to use 3-6Hz, based on the statistical analysis of the sensor-level data in
370 order to achieve the best signal-to-noise ratio for subsequent beamforming analyses.

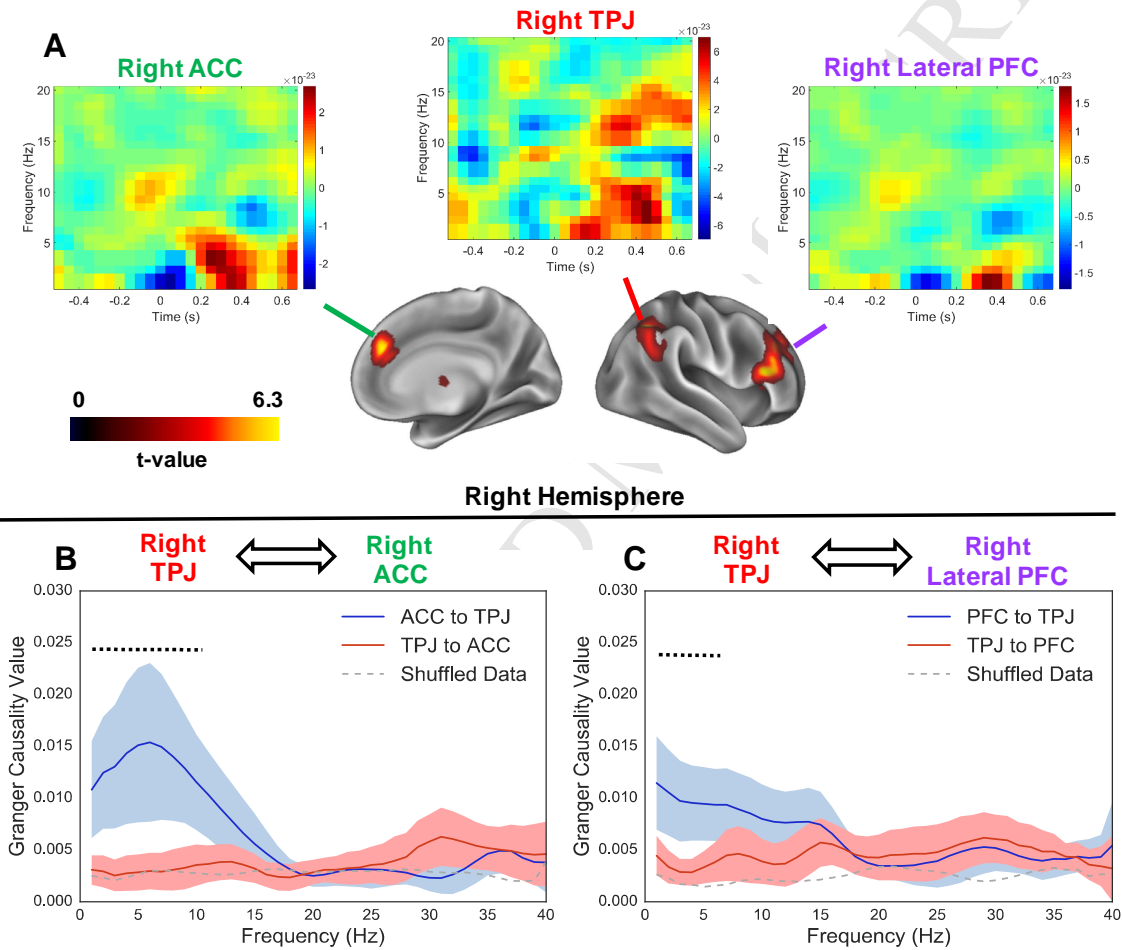
371

372 To investigate the cortical sources underlying this effect of angular disparity, theta-band (3-
373 6Hz) power was localised from 0-650ms post-stimulus onset separately for 160° and 60°
374 trials, using the Dynamic Imaging of Coherent Sources (DICS) approach (see Materials and
375 Methods). Baseline-corrected theta (3-6Hz) power was compared for LR-160 versus LR-60
376 trials and VO-160 versus VO-60 trials across a 0.8cm cortical grid (Fig. 2A; Supplementary
377 Table S3). Results showed a significant (Maris and Oostenveld 2007) ($p<.05$) increase in
378 theta power during LR-160 trials compared with LR-60 trials for right posterior temporo-
379 parietal junction (pTPJ) spreading into the inter-parietal sulcus (IPS), for right lateral pre-
380 frontal cortex (PFC) primarily overlapping with the inferior frontal gyrus (IFG) and for right
381 anterior cingulate cortex (ACC). There was also a decrease in theta power in the LR-160
382 versus LR-60 condition in the left frontal pole (Table S3).

383

384 For perspective-tracking (VO-task), there were increases in theta-power, compared with pre-
 385 trial baseline, within ventral occipital and temporo-parietal regions (Fig. S2). However, the
 386 VO-160 > VO-60 contrast showed no significant clusters (Fig. S3), indicating that angular
 387 disparity (160° versus 60°) only resulted in task-related increases in theta-band power for
 388 high-level perspective-taking and not for perspective-tracking.

389



390

391 *Figure 2:* Theta power sources and directed connectivity. Panel A depicts brain plots
 392 showing statistical results (clusters with $p < .05$ are shown) of a whole-brain DICS theta power
 393 (3-6Hz) analysis for LR-160 > LR-60 contrast visualised using the Connectome Workbench
 394 software (Van Essen et al. 2012) (see Table S3 for a complete list of power sources). Plots at
 395 the top show time-frequency representations (LR-160 > LR-60 contrast) for three virtual

396 electrodes (VE) placed in right ACC (MNI co-ordinates: [12, 36, 28]), right TPJ (MNI co-
 397 ordinates [40 -58 36]) and right lateral PFC (MNI co-ordinates: [52,32,16]). Panel B shows
 398 spectrally resolved non-parametric Granger causality (1-40Hz), computed between the right
 399 TPJ and (A) right ACC and (B) right lateral PFC, respectively. Results show an increase in
 400 Granger causality from both the right ACC (1-10Hz) and right PFC (1-5Hz) to the right TPJ.
 401 Shaded regions around each line represent 95% confidence intervals. The black dotted line
 402 above the plots represents Granger causality values passing a p<.05 threshold (see Methods
 403 for details). The grey dotted line in the plots shows shuffled data for comparison. Further
 404 explanations in the text.

405

406 [Inline supplementary material - insert Figures S2 and S3 here]

407

408 *Virtual Electrode Time-Frequency Analysis*

409 To further investigate the oscillatory signatures of high-level perspective-taking, time-courses
 410 for each trial were extracted from ‘virtual-electrodes’ in right TPJ, right ACC and right lateral
 411 PFC (see Materials & Methods for details). Low-frequency oscillatory power was then
 412 estimated between -0.65 to 0.65s post-stimulus using a Hanning taper, 0.05s sliding window.
 413 Results show very early and sustained theta power (3-6Hz) increases in the right TPJ (0-0.5s)
 414 for LR-160 versus LR-60 trials. Right lateral PFC delta/theta power (1-5Hz) and right ACC
 415 (1-5Hz) increases are more transient and begin from 0.2-0.5s post-stimulus onset. This
 416 suggests that the rTPJ is engaged throughout the process of embodied perspective-taking,
 417 whereas increases in theta power ACC and PFC occur later and more transiently.

418

419 *Granger Causality Analysis*

420 To investigate directed functional connectivity during perspective-taking between the three
 421 main regions of interest (ROIs) identified in the source power analysis (rTPJ, rACC and
 422 rPFC), we employed spectrally resolved non-parametric Granger causality (GC) on LR trials
 423 (0-0.65s post-stimulus onset) (Dhamala et al. 2008). GC is a statistical concept used to
 424 estimate directed connectivity between time-series, which relies on the premise that if the
 425 time-series of region A can be used to predict the time-series of region B, then A is said to
 426 ‘granger-cause’ B (Ding Mingzhou et al. 2006). GC can also be extended to the frequency
 427 domain (discussed further in (Bastos and Schoffelen 2016). Spectrally-resolved GC therefore
 428 provides information about the direction of connectivity between regions of interest, as well
 429 as the frequency-band underlying the effects.

430

431 Between the three ROIs, GC values showed statistically significant differences from fourier-
 432 scrambled time-series in two pairs: rTPJ-rACC and rTPJ-rPFC (Maris and Oostenveld 2007).
 433 To investigate these effects further, we statistically compared GC values between each
 434 direction of the ROI pair (i.e. the granger causal influence to and from the rTPJ). Results
 435 showed an asymmetric increase in granger causal influence, directed from right ACC
 436 between 1-10Hz, with a peak at 6Hz, (Fig. 2B, p=.009) and right PFC, between 1-6Hz, (Fig
 437 2B, p=.04) to the right TPJ.

438

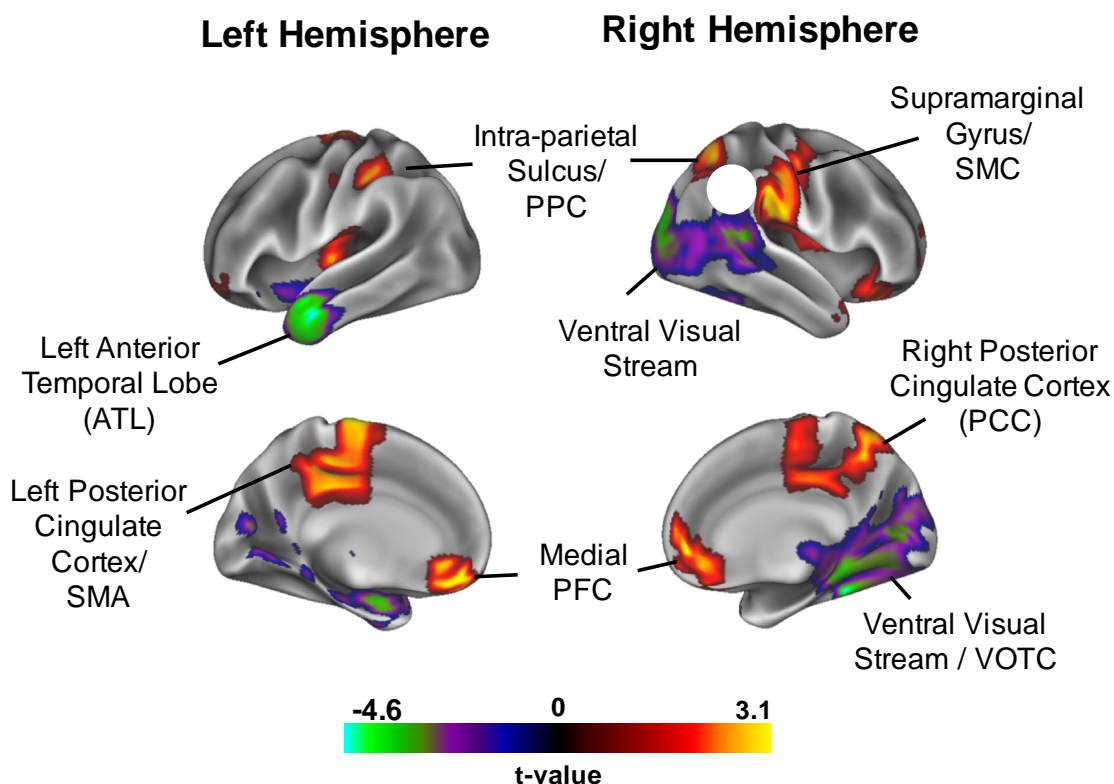
439 *Imaginary Coherence*

440 Phase-synchronised neural activity has been argued to act as a mechanism for information
 441 flow between brain regions during cognitive tasks (Womelsdorf et al. 2007). Measures of
 442 phase synchrony (e.g. coherence) can therefore provide information about changes in brain
 443 connectivity within a particular frequency band. However unlike GC, coherency alone does
 444 not provide information about the direction of connectivity.

445

446 To establish patterns of whole-brain functional connectivity accompanying right-hemisphere
 447 TPJ theta-band activity, we extracted source-level theta-band (5 ± 2 Hz) phase relationships
 448 from the sensor-level cross-spectral density matrix (see Materials and Methods). A measure
 449 of phase synchrony between a right-TPJ seed and every other voxel was calculated by
 450 projecting complex-valued coherency onto the imaginary axis (Nolte et al. 2004). The
 451 resulting coherency maps from the LR-160 and LR-60 conditions were first baseline-
 452 corrected, and then compared using cluster-based non-parametric permutation testing (Maris
 453 and Oostenveld 2007).

454



455

456 *Figure 3:* Results of a whole-brain imaginary coherence analysis in relation to a right TPJ
 457 seed (white circle) and for a LR-160 > LR-60 contrast, visualised using the Connectome
 458 Workbench software (Van Essen et al. 2012) (see Table S4 for a complete list of sources and

459 associated p-values). Clusters of coherency increase/decrease passing a $p < .05$ threshold are
 460 shown (see Material and Methods). PPC = posterior parietal cortex; SMC = sensorimotor
 461 cortex; SMA = supplementary motor area; PFC = prefrontal cortex; VOTC = ventral
 462 occipitotemporal cortex.

463

464 Results (Fig. 3) show a complex pattern of both increased and decreased theta-band phase
 465 synchrony during embodied perspective-taking. The main areas of decreased synchrony are
 466 located in the ventral occipitotemporal cortex (VOTC), overlapping with key regions of the
 467 ventral visual stream. There were also reductions in phase synchrony to the bilateral anterior
 468 temporal lobes (ATL). Increased phase synchrony was observed in bilateral medial PFC
 469 regions, posterior cingulate cortex (PCC), intra-parietal sulcus (IPS), supplementary motor
 470 area (SMA), posterior parietal cortex (PPC), and right supramarginal gyrus/sensorimotor
 471 cortex (SMC). These patterns of phase synchrony are unlikely to be driven by spurious
 472 connectivity from MEG field spread (Brookes et al. 2011), as we opted to measure imaginary
 473 coherence (Nolte et al. 2004), thereby removing effects in relation to instantaneous phase.

474

475

476 **Discussion**

477 This MEG study has investigated the oscillation-based functional connectivity between brain
 478 regions involved in our ability to take another person's visuospatial perspective. Behavioural
 479 results replicated a substantial body of research showing significantly increased reaction time
 480 for higher angular disparity between the participant and avatar (160° versus 60°) for
 481 perspective-taking but not perspective-*tracking* (Kessler and Rutherford 2010; Kessler and
 482 Thomson 2010; Surtees et al. 2013; Wang et al. 2016). Greater angular disparity for
 483 perspective-taking was accompanied by increased theta power (3-6Hz) within the right

484 TPJ/IPS and lateral PFC, replicating Wang et al., (Wang et al. 2016), as well as within the
 485 right ACC. Importantly, this increase in theta-power for angular disparity was specific to
 486 perspective-taking and not perspective-tracking (Figs. 1, S1, S3). We therefore focused on
 487 network connectivity during perspective-taking and showed (Fig. 2) that there was an
 488 increase in Granger causal influence (Dhamala et al. 2008) from lateral PFC and right ACC
 489 *to* right TPJ, but not vice-versa, mediated by low frequency brain rhythms (1-10Hz). Finally,
 490 we examined how whole-brain patterns of theta-band (5 ± 2 Hz) phase synchrony, quantified
 491 using imaginary coherence (Nolte et al. 2004), varied in relation to right TPJ activity. Results
 492 (Fig. 3) suggest that with increasing angular disparity (160° versus 60°), the right TPJ
 493 increases its phase coupling to regions involved in theory of mind (Carrington and Bailey
 494 2009) (medial PFC, PCC) and body schema (Coslett et al. 2008; Medina et al. 2009) (SMC,
 495 PPC, SMA), but decreases its phase coupling to visual regions (VOTC) and to bilateral
 496 anterior temporal lobe (ATL). Overall, these results suggest a crucial role for TPJ as a hub
 497 that functionally connects mentalizing, executive, and body-representational networks via
 498 theta-band (3-7Hz) oscillations during high-level perspective taking (Fig. 4).

499

500 *The role of the right TPJ in high-level perspective-taking*

501 Results from this study suggest that the right TPJ (rTPJ) becomes increasingly engaged with
 502 the need for embodied mental alignment during perspective-taking i.e. as the disparity grows
 503 between our own and other's perspectives (Wang et al. 2016; Gooding-Williams et al. 2017).
 504 Activity within the right TPJ is consistent with its role in establishing a sense of self (Blanke
 505 et al. 2005), and crucially in differentiating conflicts between the self and other (Santiesteban
 506 et al. 2012; Sowden and Catmur 2015; Eddy 2016). The left TPJ has also been implicated in
 507 theory of mind and perspective-taking tasks (Santiesteban et al. 2012; Schurz et al. 2013),
 508 however our results, replicating Wang et al., (2016) suggest that theta-band power is stronger

509 within the right TPJ, when there is a large angle of disparity (e.g. 160°) between self and
510 other perspective is greatest. This is consistent with some findings of lateralisation in TPJ
511 function (Igelström and Graziano 2017.). Given the importance of the rTPJ in perspective-
512 taking (Santiesteban et al. 2012; Schurz et al. 2015; Eddy 2016; Wang et al. 2016), we were
513 interested in further describing the neurocognitive processes involved.

514

515 As previous research has implicated the TPJ as a major network hub (Igelström and Graziano
516 2017.; Bzdok et al. 2013), we hypothesised that the region would co-ordinate shifts in
517 functional connectivity to other brain regions, via phase synchrony (Engel et al. 2001; Varela
518 et al. 2001). Indeed, we found that the rTPJ increased its phase-coupling to the medial PFC
519 and posterior PCC – two regions also involved more generally in understanding the mental
520 states of others (Lieberman 2007; Carrington and Bailey 2009; Van Overwalle 2009) (i.e.
521 mentalizing). Importantly, phase-coupling at theta frequency between rTPJ and medial PFC
522 had been previously reported by Bögels et al (2015) during a high-level mentalizing task.
523 Thus, TPJ-mPFC coupling could be part of a basic mechanism involved in simpler as well as
524 in more sophisticated forms of social mental alignment.

525

526 We also found increased phase synchrony between the rTPJ and SMC, SMA, and PPC (Fig.
527 3), regions previously implicated in coding for the body schema, i.e. cortical correlates of the
528 internal representation of the body and its postures and actions (Coslett et al. 2008; Medina et
529 al. 2009). We propose that this functional link, which has been reported previously (Arzy et
530 al. 2006; Cazzato et al. 2015), underlies the simulated rotation of the embodied self into
531 another's orientation and perspective, which so far has primarily been described
532 behaviourally (Kessler and Rutherford 2010; Surtees et al. 2013; Wang et al. 2016). The rTPJ
533 also showed decreased phase synchrony with visual regions (VOTC), primarily the ventral

534 stream of the right visual cortex, during high-level perspective-taking. Altogether, these
535 findings can be interpreted as an active shift from externally-driven processing (i.e. bottom-
536 up sensory information) to internal representations (i.e. self, body-schema rotation) during
537 high level perspective-taking. This switch from processing external events to updating
538 internal states and information has been previously linked with TPJ function (Bzdok et al.
539 2013; Wu et al. 2015).

540

541 Taken together, these findings suggest that rTPJ acts as a hub for high-level perspective
542 taking by routing visual information to internal representations of the self, the body and its
543 action and posture repertoire, via theta-band phase synchronisation (Figure 4). This allows
544 humans to actively project their own sense of self into another's viewpoint, resulting in rapid
545 and accurate perspective-taking responses (Kessler and Rutherford 2010; Surtees et al. 2013;
546 Wang et al. 2016; Gooding-Williams et al. 2017). However, given the simplicity of the
547 stimuli and required decisions (left or right) the social relevance of the current task and
548 associated processing could be called into question. Therefore, we would like to point out
549 that Kessler and Wang (2012) reported that social skills (social skills subscale of the AQ,
550 Baron-Cohen et al., 2001) and gender significantly predicted speed and embodiment of
551 responses on this task, suggesting that social abilities are linked to embodied perspective
552 taking even in this repetitive and simplified experimental form. Furthermore, using exactly
553 the same tasks, Kessler et al (2014, Proc R Soc B) showed that while the basic mechanisms
554 for perspective-taking and -tracking are essentially the same for Western and East-Asian
555 participants, there are subtle but significant culture-related differences in terms of self- vs.
556 other-centred biases that have been interpreted as cultural manifestations of differing social
557 norms (e.g. Markus and Kitayama, 1991; also Wu, Barr, Gann, & Keysar, 2013). Finally,
558 Bögels et al (2015) reported very similar theta oscillatory coupling between right TPJ and

559 mPFC during a more complex task of social perspective taking, where participants needed to
560 judge whether an interactor in a different room was presented with the same visual object or
561 not, based on their previous communication. This is a genuinely social task in the sense of
562 imagining another person's current visual experience with the aim to enable successful
563 communication. During this high-level social task right TPJ was phase-coherent with
564 vmPFC, thus confirming our claim that this coupling is part of the basic mechanism for
565 simpler as well as for more sophisticated forms of social mental alignment.

566

567 Interestingly, the other side of the coin of the described embodied perspective-taking process
568 tied to TPJ seems to be that aberrant activity in TPJ contributes to involuntary shifts in
569 perspective, as experienced in so-called “out-of-body” experiences (OBE) (Blanke et al.
570 2005; Kessler and Braithwaite 2016). This emerging framework is consistent with a recent
571 model arguing that the TPJ acts as a “nexus”, hub, or convergence zone between different
572 cognitive domains including social cognition, attention and executive function (Carter and
573 Huettel 2013). Our results suggest that the TPJ plays an important role during complex
574 social-cognitive processes like perspective-taking, by co-ordinating the activity between
575 multiple brain regions and functional sub-networks into a coherent whole (Santiesteban et al.
576 2012; Carter and Huettel 2013; Bögels et al. 2015; Eddy 2016) (Fig. 4). We further propose
577 that theta oscillations could be the crucial network code for this integration process (Bögels et
578 al. 2015; Wang et al. 2016; Gooding-Williams et al. 2017).

579

580 *Top-down Executive Processes during high-level perspective-taking*

581 Along with the rTPJ, two additional regions showed significantly increased theta power with
582 increasing angular disparity during perspective-taking (Fig. 2A): the lateral PFC, primarily
583 overlapping with the right inferior frontal gyrus; and the right ACC. This theta-band activity

584 was found during a slightly later period than the rTPJ, from 0.2-0.5 post-stimulus onset,
585 suggesting that the ACC and lateral PFC contribute later to the process of perspective-taking.
586 Interestingly, we also found that these two regions displayed directed functional connectivity,
587 as measured by Granger causality, to the rTPJ, mediated by low frequency brain rhythms (1-
588 10Hz), indicative of top-down processing (Von Stein et al. 2000).

589

590 Activity within the ACC and lateral PFC is typically associated with cognitive control (Aron
591 et al. 2014) and conflict monitoring (Botvinick et al. 2004). However recent work has shown
592 the regions to be also implicated in a number of theory of mind studies (Vogeley et al. 2001;
593 Hartwright et al. 2012, 2015; Samson et al. 2015). Activity within this context has been
594 argued to reflect the detection (Amodio and Frith 2006; Lieberman 2007) (ACC) and
595 resolution (Samson et al. 2005; Hartwright et al. 2012) (lateral PFC) of conflict between self
596 and other perspectives (Hartwright et al. 2016a). We therefore propose (Fig. 4) that the
597 connectivity from rACC and rPFC to rTPJ, during later stages of perspective-taking, reflects
598 domain-general “top-down” executive control processes (Duncan and Owen 2000) required
599 for suppressing the self-perspective, in favour of taking the other’s perspective (Samson et al.
600 2005; Van der Meer et al. 2011; Hartwright et al. 2015), and/or for controlling the conflict
601 between the physical self and the transformed self (the “other”) (May 2004; Santiesteban et
602 al. 2012; Wang et al. 2016), allowing both representations to co-exist in the brain, similar to
603 the experience of an OBE, where the self is located in two places at once (Kessler and
604 Braithwaite 2016). Our results differ slightly from those reported in (McClarey et al. 2011),
605 but our interpretations are not fully at odds with McClarey et al.’s, who argue that the lateral
606 PFC selects between self/other perspectives, both computed in the rTPJ, depending on task
607 demands, thus, favouring our second interpretation (i.e., ACC and lateral PFC managing the
608 conflict between self and other perspectives that may coexist in TPJ). At this stage it remains

609 unknown what information content exactly is computed in which part of the brain. Differing
610 results could also be due to differences in the paradigms employed – unlike (McCleery et al.
611 2011), perspective-taking stimuli in this study required differing levels of embodied
612 simulation, potentially requiring different levels of conflict management between self and
613 other perspectives. In addition, this study focussed on earlier frontal theta-band oscillations
614 (0-0.65s) compared with the later evoked frontal responses (0.6-0.8s) reported in (McCleery
615 et al. 2011). It should also be noted that perspective-tracking could also involve similar
616 cognitive control processes. However, the experimental contrast between different angular
617 disparities (160° vs 60°) may have precluded our ability to detect this, as similar executive
618 control processes would be equally engaged in both conditions.

619

620 More generally, whilst the involvement of executive-control processes in perspective-taking
621 is based on substantial empirical research (Aron et al. 2014; Hartwright et al. 2016a), to avoid
622 reverse-inference, future work could vary executive demands during perspective-taking
623 (Bradford et al. 2015), in combination with brain stimulation (Wang et al. 2016) to establish
624 the causal role of the lateral PFC and rACC. For example, one study has shown that theta-
625 burst TMS to lateral PFC slowed reaction times during a false belief task requiring a
626 dissociation between self and other perspectives, after modelling the structural morphology
627 of lateral PFC and right TPJ (Hartwright et al. 2016b). In addition, the observation that our
628 effects in ACC and PFC were primarily related to theta oscillations, further corroborates the
629 notion of top-down control, since theta has previously been shown to reflect top-down
630 cognitive control processes involved in conflict monitoring (Botvinick et al. 2004) and error-
631 related responses (Trujillo and Allen 2007). Our complimentary finding that the ACC and
632 lateral PFC exerted top-down influence on the TPJ via low frequency rhythms (1-10Hz,

633 peaking in theta) is clearly consistent with ACC and PFC theta as a mechanism for cognitive
634 control.

635

636 *Limitations*

637 This article, building on our previous work (Bögels et al. 2015; Wang et al. 2016; Gooding-
638 Williams et al. 2017), has focussed on the role of theta-band power and connectivity
639 underlying perspective-taking. Whilst sensor-level analysis revealed only a single positive
640 cluster of activity from 3-6Hz, corroborating our previous results, inspection of Figure 2A
641 suggests that these effects might spread into delta and low alpha frequency ranges. This is
642 also observed for right TPJ (power) and lateral PFC which peaks in delta (1-3Hz) rather than
643 theta (3-6Hz) in power and Granger causality spectra (Fig. 2). This discrepancy may explain
644 the lack of phase synchrony, probed at 5 ± 2 Hz rather than 1-3Hz, between the right TPJ and
645 lateral PFC reported using imaginary coherence. It is worth noting that the fine-grained
646 definition of frequency ranges is confounded by spectral smoothing applied during the
647 frequency decomposition process. Future work should therefore attempt to clarify whether
648 there might be additional independent or multiplexed oscillatory networks (e.g. Seymour et
649 al. 2017) at different frequency ranges, including those between delta/theta and gamma
650 (>30Hz) bands (Cao et al. 2018). Nevertheless, this article suggests that theta (3-6Hz)
651 appears to be the most dominant oscillatory frequency band (if not the only band), underlying
652 embodied perspective-taking.

653

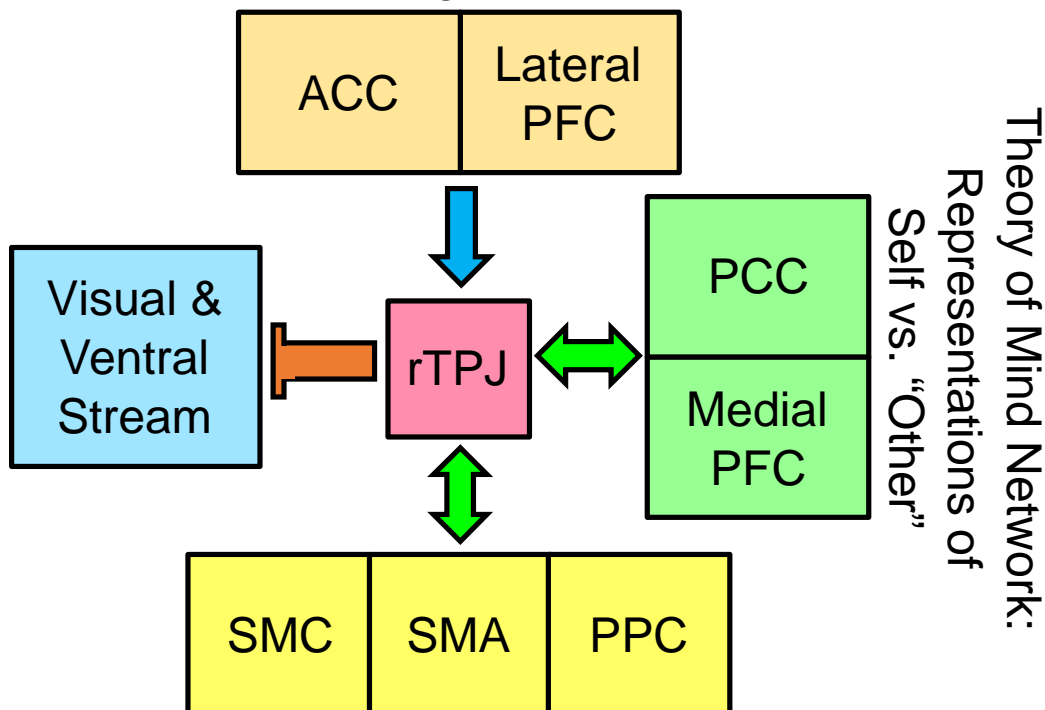
654 *Conclusion*

655 This study examined the cortical networks involved in high-level mental alignment
656 (perspective taking), co-ordinated by theta-band oscillations. Low-frequency phase coupling
657 in the theta-band, has previously been shown to contribute to the co-ordination of long-range

658 neuronal interactions (von Stein and Sarnthein 2000; Mizuhara et al. 2004), through which
 659 distributed neural assemblies become integrated into a coherent network (Varela et al. 2001).
 660 Our finding that theta-band phase-coupling synchronises the right temporo-parietal junction
 661 (rTPJ) to brain regions involved in theory of mind and regions coding for body schema
 662 supports this view, and suggests that perspective taking, and potentially other social cognitive
 663 processes, involve the co-ordination of spatially and functionally disperse brain regions via
 664 theta-band phase synchrony (von Stein and Sarnthein 2000), further supported by low-
 665 frequency top-down influences from executive control areas (Bögels et al. 2015).

666

Executive Network: Top-down Cognitive Control



Motor/Body-Schema Network: Embodied Transformation

667

668 *Figure 4:* Proposed network underlying high-level perspective-taking (Kessler and
 669 Rutherford 2010; Surtees et al. 2013), linked by power and phase in the theta-band (3-7Hz).

670 During initiation of embodied perspective-taking behaviour, early rTPJ activity co-ordinates
671 connectivity decreases with visual regions, whilst increasing connectivity with regions
672 involved in Theory of Mind, and Motor/Body-Schema. Increases in low frequency (primarily
673 theta) power within the lateral PFC and ACC reflect domain-general cognitive control
674 processes for detecting and managing top-down the conflict between self and other
675 perspectives.

676

677 **Acknowledgements**

678 We wish to thank Gerard Gooding-Williams for MRI acquisition and the Wellcome and Dr.
679 Hadwen Trusts for supporting MEG scanning costs. RS was supported by a Cotutelle Ph.D.
680 studentship from Aston University and Macquarie University.

681

682 **References:**

- 683 Amodio DM, Frith CD. 2006. Meeting of minds: the medial frontal cortex and social
684 cognition. Nat Rev Neurosci. 7:268.
- 685 Aron AR, Robbins TW, Poldrack RA. 2014. Inhibition and the right inferior frontal cortex:
686 one decade on. Trends Cogn Sci. 18:177–185.
- 687 Arzy S, Thut G, Mohr C, Michel CM, Blanke O. 2006. Neural Basis of Embodiment: Distinct
688 Contributions of Temporoparietal Junction and Extrastriate Body Area. J Neurosci.
689 26:8074–8081.
- 690 Baron-Cohen S, Wheelwright S, Skinner R, Martin J, & Clubley, E. 2001. The autism-
691 spectrum quotient (AQ): Evidence from asperger syndrome/high-functioning autism,
692 males and females, scientists and mathematicians. Journal of autism and
693 developmental disorders, 31:1, 5-17.

- 694 Bastos AM, Schoffelen J-M. 2016. A Tutorial Review of Functional Connectivity Analysis
695 Methods and Their Interpretational Pitfalls. *Front Syst Neurosci.* 175.
- 696 Blanke O, Mohr C, Michel CM, Pascual-Leone A, Brugger P, Seeck M, Landis T, Thut G.
697 2005. Linking out-of-body experience and self processing to mental own-body
698 imagery at the temporoparietal junction. *J Neurosci.* 25:550–557.
- 699 Bögels S, Barr DJ, Garrod S, Kessler K. 2015. Conversational interaction in the scanner:
700 mentalizing during language processing as revealed by MEG. *Cereb Cortex.* 25:3219–
701 3234.
- 702 Botvinick MM, Cohen JD, Carter CS. 2004. Conflict monitoring and anterior cingulate
703 cortex: an update. *Trends Cogn Sci.* 8:539–546.
- 704 Bradford EEF, Jentzsch I, Gomez J-C. 2015. From self to social cognition: Theory of Mind
705 mechanisms and their relation to Executive Functioning. *Cognition.* 138:21–34.
- 706 Bräuer J, Call J, Tomasello M. 2007. Chimpanzees really know what others can see in a
707 competitive situation. *Anim Cogn.* 10:439–448.
- 708 Brookes MJ, Hale JR, Zumer JM, Stevenson CM, Francis ST, Barnes GR, Owen JP, Morris
709 PG, Nagarajan SS. 2011. Measuring functional connectivity using MEG:
710 methodology and comparison with fcMRI. *Neuroimage.* 56:1082–1104.
- 711 Bugnyar T, Stöwe M, Heinrich B. 2004. Ravens, Corvus corax, follow gaze direction of
712 humans around obstacles. *Proc R Soc Lond B Biol Sci.* 271:1331–1336.
- 713 Bzdok D, Langner R, Schilbach L, Jakobs O, Roski C, Caspers S, Laird AR, Fox PT, Zilles
714 K, Eickhoff SB. 2013. Characterization of the temporo-parietal junction by combining
715 data-driven parcellation, complementary connectivity analyses, and functional
716 decoding. *NeuroImage.* 81:381–392.
- 717 Call J, Tomasello M. 1999. A nonverbal false belief task: The performance of children and
718 great apes. *Child Dev.* 70:381–395.

- 719 Cao W, Lin S, Xia Q, Du Y, Yang Q, Zhang M, Lu Y, Xu J, Duan S, Xia J, Feng G, Xu J,
720 Luo J. 2018. Gamma Oscillation Dysfunction in mPFC Leads to Social Deficits in
721 Neuroligin 3 R451C Knockin Mice. *Neuron*. 97:1253-1260.e7.
- 722 Carrington SJ, Bailey AJ. 2009. Are there theory of mind regions in the brain? A review of
723 the neuroimaging literature. *Hum Brain Mapp*. 30:2313–2335.
- 724 Carter RM, Huettel SA. 2013. A nexus model of the temporal–parietal junction. *Trends Cogn
725 Sci*. 17:328–336.
- 726 Cazzato V, Mian E, Serino A, Mele S, Urgesi C. 2015. Distinct contributions of extrastriate
727 body area and temporoparietal junction in perceiving one's own and others' body.
728 *Cogn Affect Behav Neurosci*. 15:211–228.
- 729 Coslett H, Buxbaum LJ, Schwoebel J. 2008. Accurate reaching after active but not passive
730 movements of the hand: Evidence for forward modeling. *Behav Neurol*. 19:117–125.
- 731 Dhamala M, Rangarajan G, Ding M. 2008. Analyzing information flow in brain networks
732 with nonparametric Granger causality. *Neuroimage*. 41:354–362.
- 733 Ding Mingzhou, Chen Yonghong, Bressler Steven L. 2006. Granger Causality: Basic Theory
734 and Application to Neuroscience. *Handb Time Ser Anal*, Wiley Online Books.
- 735 Duncan J, Owen AM. 2000. Common regions of the human frontal lobe recruited by diverse
736 cognitive demands. *Trends Neurosci*. 23:475–483.
- 737 Eddy CM. 2016. The junction between self and other? Temporo-parietal dysfunction in
738 neuropsychiatry. *Neuropsychologia*. 89:465–477.
- 739 Engel AK, Fries P, Singer W. 2001. Dynamic predictions: Oscillations and synchrony in top–
740 down processing. *Nat Rev Neurosci*. 2:704–716.
- 741 Flavell JH, Everett BA, Croft K, Flavell ER. 1981. Young children's knowledge about visual
742 perception: Further evidence for the Level 1–Level 2 distinction. *Dev Psychol*. 17:99.
- 743 Frith CD, Frith U. 2007. Social cognition in humans. *Curr Biol*. 17:R724–R732.

- 744 Garcia D. 2010. Robust smoothing of gridded data in one and higher dimensions with
 745 missing values. *Comput Stat Data Anal.* 54:1167–1178.
- 746 Gooding-Williams G, Wang H, Kessler K. 2017. THETA-Rhythm Makes the World Go
 747 Round: Dissociative Effects of TMS Theta Versus Alpha Entrainment of Right pTPJ
 748 on Embodied Perspective Transformations. *Brain Topogr.* 1–4.
- 749 Gross s J, Kujala J, Hämäläinen M, Timmermann L, Schnitzler A, Salmelin R. 2001.
 750 Dynamic imaging of coherent sources: studying neural interactions in the human
 751 brain. *Proc Natl Acad Sci.* 98:694–699.
- 752 Gzesh SM, Surber CF. 1985. Visual perspective-taking skills in children. *Child Dev.* 1204–
 753 1213.
- 754 Hartwright CE, Apperly IA, Hansen PC. 2012. Multiple roles for executive control in belief–
 755 desire reasoning: Distinct neural networks are recruited for self perspective inhibition
 756 and complexity of reasoning. *NeuroImage.* 61:921–930.
- 757 Hartwright CE, Apperly IA, Hansen PC. 2015. The special case of self-perspective inhibition
 758 in mental, but not non-mental, representation. *Neuropsychologia.* 67:183–192.
- 759 Hartwright CE, Hansen PC, Apperly IA. 2016a. Current knowledge on the role of the Inferior
 760 Frontal Gyrus in Theory of Mind – A commentary on Schurz and Tholen (2016).
 761 *Cortex.* 85:133–136.
- 762 Hartwright Charlotte E., Hardwick Robert M., Apperly Ian A., Hansen Peter C. 2016b.
 763 Resting state morphology predicts the effect of theta burst stimulation in false belief
 764 reasoning. *Hum Brain Mapp.* 37:3502–3514.
- 765 Igelström KM, Graziano MSA. 2017. The inferior parietal lobule and temporoparietal
 766 junction: A network perspective. *Neuropsychologia.*
- 767 Jenkinson M, Smith S. 2001. A global optimisation method for robust affine registration of
 768 brain images. *Med Image Anal.* 5:143–156.

- 769 Kessler K, Braithwaite JJ. 2016. Deliberate and spontaneous sensations of disembodiment:
 770 capacity or flaw? *Cognit Neuropsychiatry*. 21:412–428.
- 771 Kessler K, Cao L, O'Shea K J, Wang H. 2014. A cross-culture, cross-gender comparison of
 772 perspective taking mechanisms. *Proceedings of the Royal Society of London B:*
 773 Biological Sciences, 281:1785, 20140388.
- 774 Kessler K, Rutherford H. 2010. The Two Forms of Visuo-Spatial Perspective Taking are
 775 Differently Embodied and Subserve Different Spatial Prepositions. *Front Psychol.*
 776 1:213.
- 777 Kessler K, Thomson LA. 2010. The embodied nature of spatial perspective taking: embodied
 778 transformation versus sensorimotor interference. *Cognition*. 114:72–88.
- 779 Kessler, K, Wang, H. 2012. Spatial perspective taking is an embodied process, but not for
 780 everyone in the same way: differences predicted by sex and social skills score. *Spatial*
 781 *Cog & Comp*, 12:2-3, 133-158.
- 782 Lieberman MD. 2007. Social cognitive neuroscience: a review of core processes. *Annu Rev*
 783 *Psychol.* 58:259–289.
- 784 Lombardo MV, Chakrabarti B, Bullmore ET, Wheelwright SJ, Sadek SA, Suckling J, Baron-
 785 Cohen S, Consortium MA, others. 2010. Shared neural circuits for mentalizing about
 786 the self and others. *J Cogn Neurosci*. 22:1623–1635.
- 787 Maris E, Oostenveld R. 2007. Nonparametric statistical testing of EEG- and MEG-data. *J*
 788 *Neurosci Methods*. 164:177–190.
- 789 Markus HR, Kitayama S. 1991. Culture and the self: Implications for cognition, emotion,
 790 and motivation. *Psychological review*, 98:2, 224.
- 791 Mars RB, Sallet J, Schüffelgen U, Jbabdi S, Toni I, Rushworth MF. 2012. Connectivity-
 792 based subdivisions of the human right “temporoparietal junction area”: evidence for

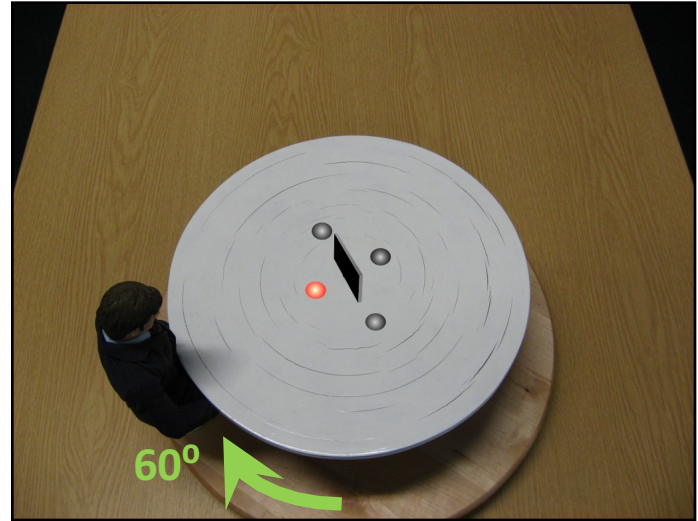
- 793 different areas participating in different cortical networks. *Cereb Cortex.* 22:1894–
794 1903.
- 795 May M. 2004. Imaginal perspective switches in remembered environments: Transformation
796 versus interference accounts. *Cognit Psychol.* 48:163–206.
- 797 McCleery JP, Surtees ADR, Graham KA, Richards JE, Apperly IA. 2011. The Neural and
798 Cognitive Time Course of Theory of Mind. *J Neurosci.* 31:12849–12854.
- 799 Medina J, Jax SA, Coslett HB. 2009. Two-component models of reaching: Evidence from
800 deafferentation in a Fitts' law task. *Neurosci Lett.* 451:222–226.
- 801 Mizuhara H, Wang L-Q, Kobayashi K, Yamaguchi Y. 2004. A long-range cortical network
802 emerging with theta oscillation in a mental task. *Neuroreport.* 15:1233–1238.
- 803 Moll H, Tomasello M. 2006. Level 1 perspective-taking at 24 months of age. *Br J Dev
804 Psychol.* 24:603–613.
- 805 Nolte G. 2003. The magnetic lead field theorem in the quasi-static approximation and its use
806 for magnetoencephalography forward calculation in realistic volume conductors. *Phys
807 Med Biol.* 48:3637–3652.
- 808 Nolte G, Bai O, Wheaton L, Mari Z, Vorbach S, Hallett M. 2004. Identifying true brain
809 interaction from EEG data using the imaginary part of coherency. *Clin Neurophysiol
810 Off J Int Fed Clin Neurophysiol.* 115:2292–2307.
- 811 Oostenveld R, Fries P, Maris E, Schoffelen J-M. 2010. FieldTrip: open source software for
812 advanced analysis of MEG, EEG, and invasive electrophysiological data. *Comput
813 Intell Neurosci.* 2011.
- 814 Povinelli DJ, Bering JM, Giambrone S. 2000. Toward a science of other minds: Escaping the
815 argument by analogy. *Cogn Sci.* 24:509–541.
- 816 Samson D, Apperly IA, Kathirgamanathan U, Humphreys GW. 2005. Seeing it my way: a
817 case of a selective deficit in inhibiting self-perspective. *Brain.* 128:1102–1111.

- 818 Samson D, Houthuys S, Humphreys GW. 2015. Self-perspective inhibition deficits cannot be
819 explained by general executive control difficulties. *Cortex*. 70:189–201.
- 820 Santiesteban I, Banissy MJ, Catmur C, Bird G. 2012. Enhancing social ability by stimulating
821 right temporoparietal junction. *Curr Biol*. 22:2274–2277.
- 822 Schurz M, Aichhorn M, Martin A, Perner J. 2013. Common brain areas engaged in false
823 belief reasoning and visual perspective taking: a meta-analysis of functional brain
824 imaging studies. *Front Hum Neurosci*. 7.
- 825 Schurz M, Kronbichler M, Weissengruber S, Surtees A, Samson D, Perner J. 2015.
826 Clarifying the role of theory of mind areas during visual perspective taking: Issues of
827 spontaneity and domain-specificity. *NeuroImage*. 117:386–396.
- 828 Seymour RA. 2017. Neurofractal/perspective_taking_oscillatory_networks: Work in Progress
829 Release of Perspective Taking Data.
- 830 Seymour RA, Rippon G, Kessler K. 2017. The Detection of Phase Amplitude Coupling
831 during Sensory Processing. *Front Neurosci*. 11:487.
- 832 Sowden S, Catmur C. 2015. The role of the right temporoparietal junction in the control of
833 imitation. *Cereb Cortex*. 25:1107–1113.
- 834 Surtees A, Apperly I, Samson D. 2013. The use of embodied self-rotation for visual and
835 spatial perspective-taking. *Front Hum Neurosci*. 7.
- 836 Tomasello M, Carpenter M, Call J, Behne T, Moll H. 2005. Understanding and sharing
837 intentions: the origins of cultural cognition. *Behav Brain Sci*. 28:675–691; discussion
838 691-735.
- 839 Trujillo LT, Allen JJ. 2007. Theta EEG dynamics of the error-related negativity. *Clin
840 Neurophysiol*. 118:645–668.

- 841 Van der Meer L, Groenewold NA, Nolen WA, Pijnenborg M, Aleman A. 2011. Inhibit
842 yourself and understand the other: neural basis of distinct processes underlying
843 Theory of Mind. *Neuroimage*. 56:2364–2374.
- 844 Van Essen DC, Ugurbil K, Auerbach E, Barch D, Behrens TEJ, Bucholz R, Chang A, Chen
845 L, Corbetta M, Curtiss SW, others. 2012. The Human Connectome Project: a data
846 acquisition perspective. *Neuroimage*. 62:2222–2231.
- 847 Van Overwalle F. 2009. Social cognition and the brain: A meta-analysis. *Hum Brain Mapp*.
848 30:829–858.
- 849 Van Overwalle F. 2011. A dissociation between social mentalizing and general reasoning.
850 *Neuroimage*. 54:1589–1599.
- 851 Van Overwalle F, Baetens K. 2009. Understanding others' actions and goals by mirror and
852 mentalizing systems: a meta-analysis. *Neuroimage*. 48:564–584.
- 853 Varela F, Lachaux J-P, Rodriguez E, Martinerie J. 2001. The brainweb: phase
854 synchronization and large-scale integration. *Nat Rev Neurosci*. 2:229–239.
- 855 Vincent JL, Kahn I, Snyder AZ, Raichle ME, Buckner RL. 2008. Evidence for a
856 frontoparietal control system revealed by intrinsic functional connectivity. *J*
857 *Neurophysiol*. 100:3328–3342.
- 858 Vogeley K, Bussfeld P, Newen A, Herrmann S, Happé F, Falkai P, Maier W, Shah NJ, Fink
859 GR, Zilles K. 2001. Mind reading: neural mechanisms of theory of mind and self-
860 perspective. *Neuroimage*. 14:170–181.
- 861 Von Stein A, Chiang C, König P. 2000. Top-down processing mediated by interareal
862 synchronization. *Proc Natl Acad Sci*. 97:14748–14753.
- 863 von Stein A, Sarnthein J. 2000. Different frequencies for different scales of cortical
864 integration: from local gamma to long range alpha/theta synchronization. *Int J*
865 *Psychophysiol*. 38:301–313.

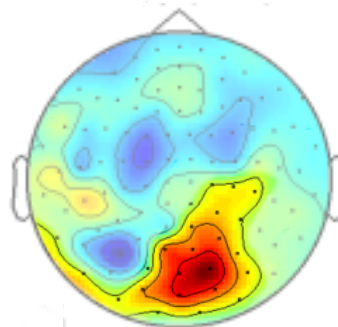
- 866 Wang H, Callaghan E, Gooding-Williams G, McAllister C, Kessler K. 2016. Rhythm makes
867 the world go round: An MEG-TMS study on the role of right TPJ theta oscillations in
868 embodied perspective taking. *Cortex J Devoted Study Nerv Syst Behav.* 75:68–81.
- 869 Womelsdorf T, Schoffelen J-M, Oostenveld R, Singer W, Desimone R, Engel AK, Fries P.
870 2007. Modulation of neuronal interactions through neuronal synchronization. *Science.*
871 316:1609–1612.
- 872 Wu S, Barr DJ, Gann TM, Keysar B. 2013. How culture influences perspective taking:
873 differences in correction, not integration. *Frontiers in human neuroscience,* 7, 822.
- 874 Wu Q, Chang C-F, Xi S, Huang I-W, Liu Z, Juan C-H, Wu Y, Fan J. 2015. A critical role of
875 temporoparietal junction in the integration of top-down and bottom-up attentional
876 control. *Hum Brain Mapp.* 36:4317–4333.
- 877 Zacks JM, Michelon P. 2005. Transformations of visuospatial images. *Behav Cogn Neurosci*
878 *Rev.* 4:96–118.
- 879

“left or right?”

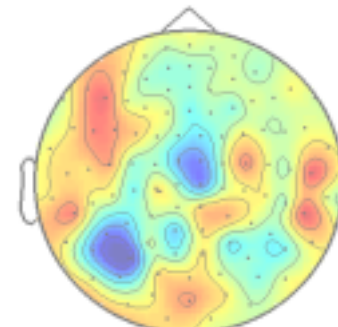


“visible or occluded?”

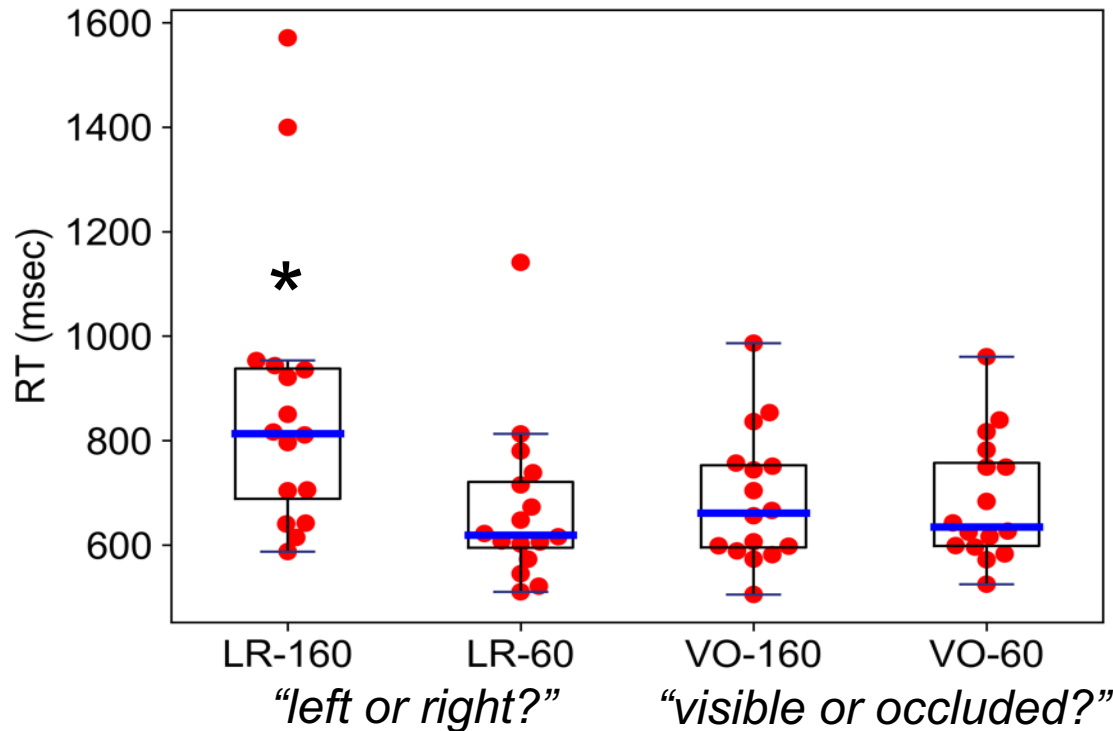
Theta 3-6Hz; 0-650ms post-stimulus onset

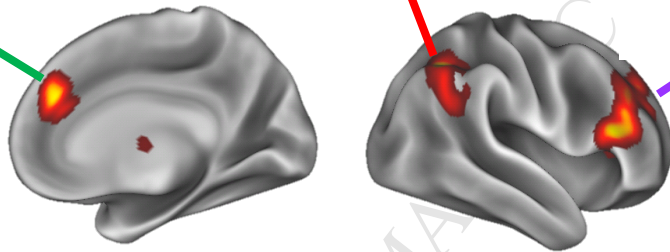
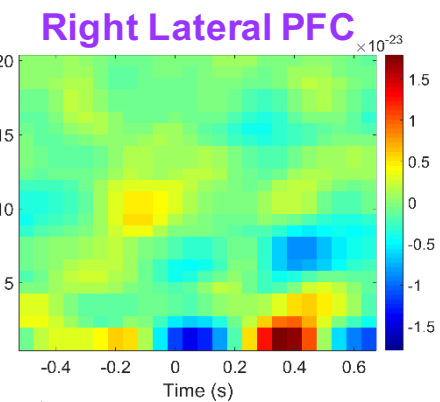
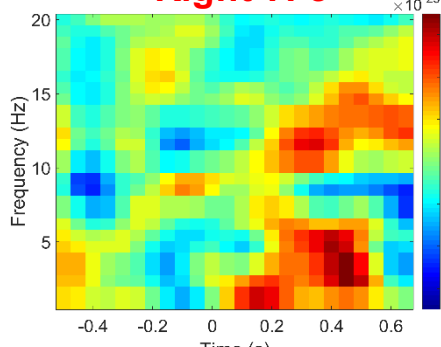
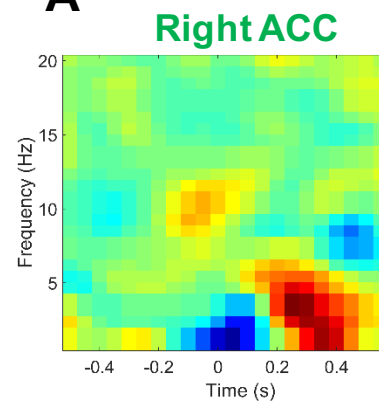


LR-160 > LR-60



VO-160 > VO-60



A

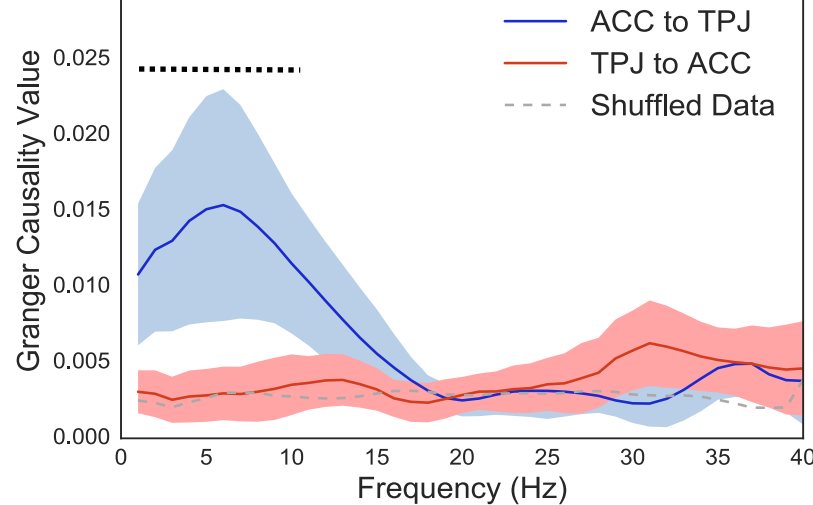
Right Hemisphere

B

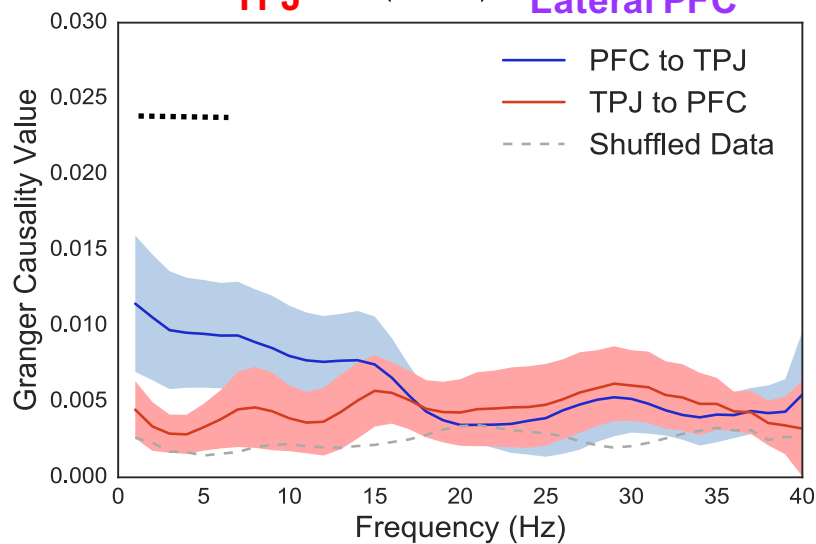
Right
TPJ ↔ Right
ACC

C

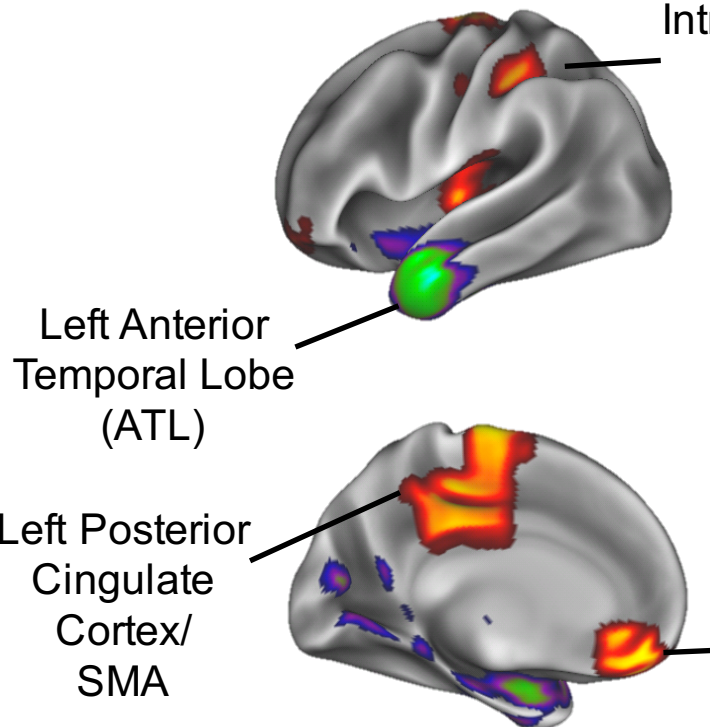
Right
TPJ ↔ Right
Lateral PFC



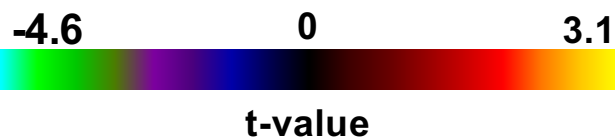
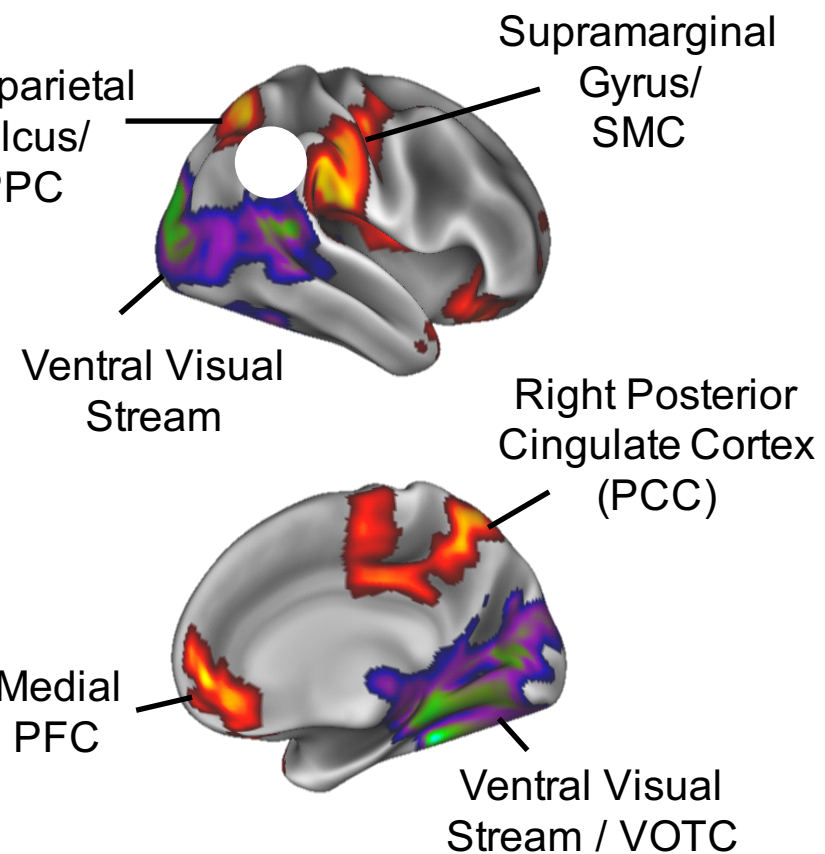
C



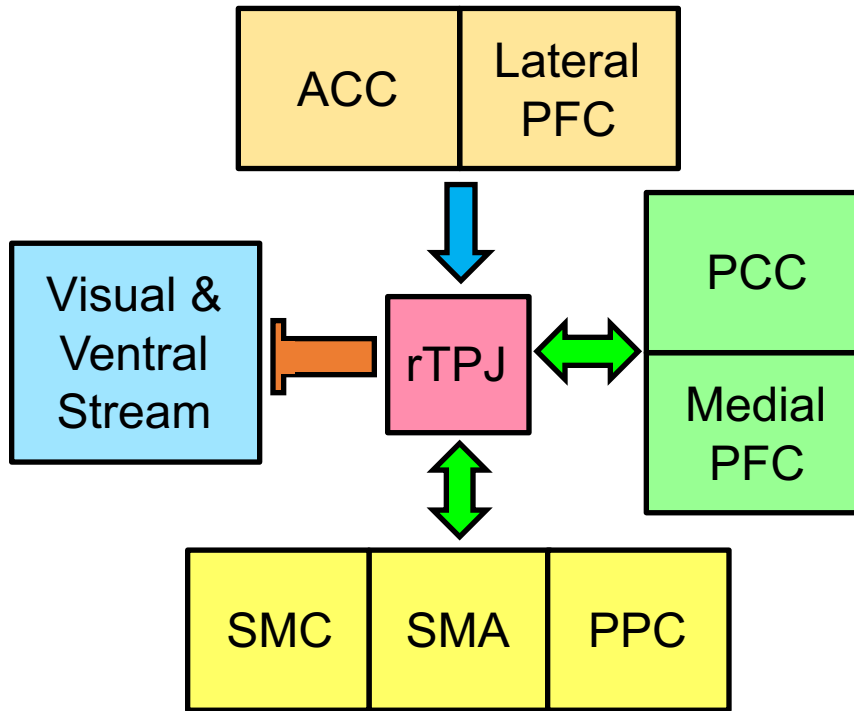
Left Hemisphere



Right Hemisphere



Executive Network: Top-down Cognitive Control



Theory of Mind Network:
Representations of
Self vs. "Other",

Motor/Body-Schema Network: Embodied Transformation